

A novel non-enzymatic lindane sensor based on CuO-MnO₂ hierarchical nano-microstructures for enhanced sensitivity

Anu Prathap, Mylamparambil Udayan; Sun, Shengnan; Wei, Chao; Xu, Zhichuan Jason

2015

Anu Prathap, M. U., Sun, S., Wei, C., & Xu, Z. J. (2015). A novel non-enzymatic lindane sensor based on CuO-MnO₂ hierarchical nano-microstructures for enhanced sensitivity. *Chemical communications*, 51(21), 4376-4379.

<https://hdl.handle.net/10356/81655>

<https://doi.org/10.1039/C5CC00024F>

© 2015 The Author(s). This is the author created version of a work that has been peer reviewed and accepted for publication in *Chemical Communications*, published by Royal Society of Chemistry on behalf of The Author(s). It incorporates referee's comments but changes resulting from the publishing process, such as copyediting, structural formatting, may not be reflected in this document. The published version is available at: [<http://dx.doi.org/10.1039/C5CC00024F>].

Downloaded on 11 Sep 2024 22:18:02 SGT

COMMUNICATION

A novel non-enzymatic lindane sensor based on CuO/MnO₂ hierarchical nano-microstructures for enhanced sensitivity

Cite this: DOI: 10.1039/x0xx00000x

M.U. Anu Prathap, Shengnan Sun, Chao Wei and Zhichuan J. Xu *

Received 00th January 2012,

Accepted 00th January 2012

DOI: 10.1039/x0xx00000x

www.rsc.org/

In this work, we present new results about the non-enzymatic detection of lindane by using CuO/MnO₂ hierarchical nano-microstructure. The linear range for the determination of lindane is up to 700 μM with a limit of detection of 4.8 nM which is much lower than for other non-enzymatic lindane sensors.

In 1825, Michael Faraday reported to the Royal Society of London the synthesis and isolation of hexachlorocyclohexane (HCCH), otherwise known as benzene hexachloride.¹ The reaction generates stereoisomers of HCCH, among these isomers, only the Lindane (γ-HCCH) exhibits insecticidal property.¹ Lindane has been used worldwide as a general, broad-spectrum insecticide for a variety of purposes, including fumigation of stored grain products, pest control on domestic animals, mosquito control, to kill soil-dwelling and plant-eating insects.^{2,3} Many countries have been using γ-HCCH as a topical treatment for head lice and scabies. Lindane is not bio-degradable; therefore, its accumulation has been detected in human blood, breast milk, and adipose tissue around the world.^{2,3} As a consequence of its toxic, carcinogenic, bioaccumulative and suspected endocrine disrupting properties, γ-HCCH was listed in 2009 as persistent organic pollutants (POPs) by the Stockholm Convention.⁴ For this reason, research and development into new techniques for the degradation of lindane by various methods of dechlorination has attracted a great deal of interest over recent years.⁵ Presently, analysis of organohalide contamination often relies on the sophisticated analytical techniques such as gas chromatography, liquid chromatography or gas chromatography–mass spectrometry (GC–MS).⁶ The overall analytical process is complex, expensive, and relies on skillful manpower. Therefore, a simple method for sensitive and selective detection of lindane is highly desirable. Electrochemical biosensors are promising alternatives to conventional analytical tools since they offer a rapid, specific, and sensitive protocol for the detection of environmental pollutants, including pesticides.⁷ A major limitation for the development of γ-HCCH biosensor is the availability of bioreceptor probe, which can specifically detect the target analyte.⁷ Lindane is insoluble in water and has a very high reduction potential, the direct reduction of lindane using the aqueous medium is a challenging task. Polarographic study in ethanol/water; γ-HCCH gave only one reduction wave and it has been concluded that the reduction takes place through a six-electron transfer process to form benzene.⁸ It has been known that certain metals, notably nickel, manganese and

cobalt, can catalyze, the reduction of organohalides at much more moderate potentials.^{8,9} The overall reaction is $RX + H^+ + 2e^- \rightarrow RH + X^-$. The source of electrons for these reactions may be either chemical or electrochemical.⁹ Metal and transition metal oxide nanoparticles have emerged as a viable alternative in fabricating highly efficient non-enzymatic electrochemical sensors.¹⁰ In particular, MnO₂ and CuO nanomaterials are considered as one of the most appealing inorganic materials and have drawn attention in bioanalytical chemistry, especially in electrochemical sensing.¹⁰ Researchers have recognized that metal oxides composites always show excellent electrochemical performances over the single metal oxide alone.^{10a,c} Therefore, a facile route for large-scale production of CuO/MnO₂ composites is still highly demanded.

In this communication, we report a facile method for the synthesis of CuO/MnO₂ hierarchical nano-microstructure. Further, we demonstrated the applicability of CuO/MnO₂ hierarchical nano-microstructure as an active electrocatalyst towards reduction of lindane. The CuO/MnO₂ sensors exhibited low detection limit, and wide linear range toward the detection of lindane, which can be ascribed to the novel structure of CuO/MnO₂ composites.

Materials prepared in this study were subjected to XRD investigation (Fig. 1a). XRD pattern of the CuO can be indexed to monoclinic CuO (JCPDS 41.0254) and that of MnO₂, can be indexed to monoclinic K-birnessite (JCPDS no. 80-1098) (Fig. 1a). The diffraction peaks from both CuO and K-birnessite MnO₂ are clearly observed in the XRD pattern of CuO/MnO₂. In the XRD pattern of the CuO/MnO₂ composites, several diffraction peaks from the CuO have disappeared due to the thick coating of the MnO₂ (Fig.

1a). FESEM and TEM images are presented in Fig. 1b-d. Clearly, CuO are made up of a great number of leaves like structures (Fig.

1b). The FESEM image of MnO₂ is shown in Fig. 1c, which clearly illustrates the nanostructured hierarchical flower-like morphology. FESEM image of CuO/MnO₂ revealed that CuO had been homogeneously wrapped with a layer of dense MnO₂ nanoflakes (Fig. 1d). From TEM image (Fig. 1d, inset), clearly the MnO₂ nanoflakes are interconnected and quite uniformly grown over the surface of the CuO, forming an attractive porous heterostructure. HRTEM images of the CuO/MnO₂ (Fig. S1, ESI†), indicate that porous MnO₂ layer are composed of numerous tiny nanoflakes.

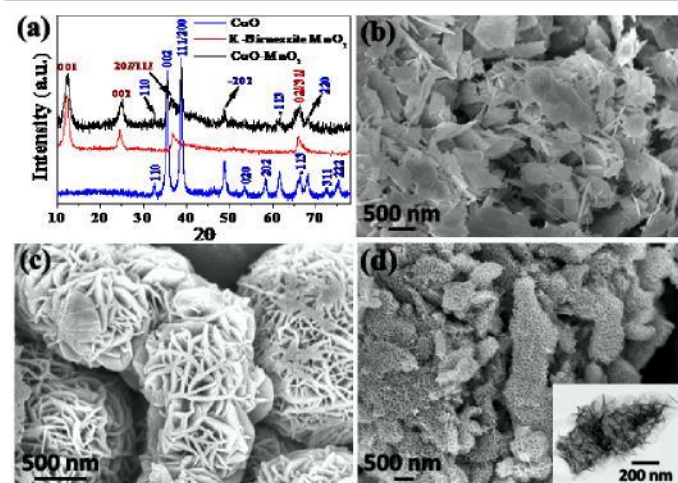


Fig. 1 (a) XRD patterns of materials synthesized in this study. SEM images of CuO (b), MnO₂ (c), CuO/MnO₂ (d); the inset show the corresponding TEM image of CuO/MnO₂.

The textural properties of metal oxides were investigated by N₂ adsorption/desorption measurements (Fig. S2, ESI†). CuO/MnO₂ exhibits type IV isotherm with H3 hysteresis loop. The increase in slope at 0.45 corresponds to capillary condensation, typical of mesoporous materials, while the further increase at higher relative pressures indicates inter-particle porosity with slit-shaped pores.^{10b,c} BJH pore size distribution of CuO/MnO₂ shows a pore size distribution centered at ~22.7 nm (Fig. S2, inset). The surface areas of 31.3, 55, and 77.6 m²/g and pore volumes of 0.112, 0.15, and 0.157 cm³/g were obtained for CuO, MnO₂, and CuO/MnO₂, respectively. To investigate surface property of the composite, FT-IR spectrum analysis was conducted (Fig. S3, ESI†). Samples show characteristic absorption bands in the range of 400 to 800 cm⁻¹, which can be assigned to Mn–O stretching vibrations (Fig. S3, ESI†).^{10b} The FT-IR spectra of CuO/MnO₂ exhibited very weak signals corresponding to the vibrational modes of CuO due to the high loading of MnO₂.^{10b} Diffused reflectance UV–visible investigation was used to determine the electronic structure and optical properties of CuO/MnO₂ (Fig. S4, ESI†). The band gap value for the CuO was found to be 1.6 eV.¹¹ The observed optical band gap for CuO/MnO₂ was found to be 1.91 eV. Furthermore, the increase in the optical band gap in CuO/MnO₂ materials can be explained on the basis of quantum size effect.¹¹ The study suggests that MnO₂ acted as a chemical modifier and caused a structural change or electronic effect.

CuO/MnO₂ modified electrode was constructed to obtain the optimized analysis parameter for lindane reduction. Fig. S5 (ESI†) shows cyclic voltammetric responses at the CuO/MnO₂ modified electrode before and after the addition of lindane (200 μM). In the absence of lindane, no peak was observed. When lindane was added, a distinct peak at -1.5 V (vs Ag/AgCl) appeared, which is completely irreversible, imply that the reaction with lindane at CuO/MnO₂ modified electrode is rapid (Fig. S5, ESI†).^{8c-e} The effect of potential scan rate on the reduction peak currents was investigated in the range from 20 to 300 mV s⁻¹ (Fig. S6, ESI†). Reduction peak currents are linearly proportional to the square root of the scan rate, which shows that lindane undergoes a diffusion controlled reduction; the non-zero intercept can be explained as an adsorption process after diffusion to the electrode surface (Fig. S6, ESI†).^{8c-g} The results of the voltammetric analyses are collected in Table S1. A survey of the data reported in Table S1 showed that the transfer coefficient (α) value less than 0.5. It is well established that dissociative electron transfer (ET) which is concerted has a very small value of α typically

around 0.3.¹² Moreover, there is no reverse peak obtained for a wide range of scan rates, which shows that the reduction process is irreversible.¹² The removal of a chlorine atom by the reduction of polychlorinated benzenes always leads to a product that is more difficult to reduce.¹³ In contrast, cleavage of carbon–chlorine bonds in lindane take place very fast and readily form fully reduced benzene.¹³ Differential pulse voltammetric (DPV) response at CuO/MnO₂ modified electrode for different concentrations of lindane is shown in Fig. 2. The current obtained is proportional to the concentration of lindane in the reaction vessel (Fig. 2, inset).

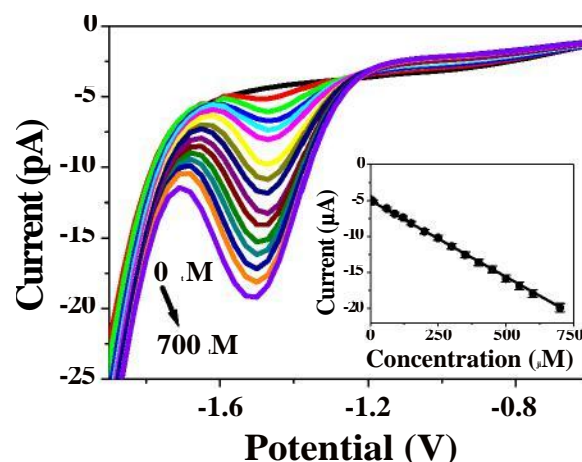


Fig. 2 DPVs of lindane at varying concentrations at the CuO/MnO₂ modified electrode using 0.05 M TBAB solution in 60:40 methanol–water (20 mL). Inset shows the calibration plot. DPV parameters were selected as: peak height = 50 mV; peak width = 200 ms; peak period = 400 ms; increment = 20 mV; pre and post-pulse width = 3 ms.

A linear response was obtained between the peak current and lindane concentration (Fig. 2) with linear regression equation of, $I(\mu\text{A}) = -4.18 - 0.022C$ ($\mu\text{mol L}^{-1}$) ($R^2 = 0.9998$) in the concentration range of 1 μM–700 μM with the sensitivity of 0.12 μA μM⁻¹ cm² and a lower detection limit of 4.8 nM. DPV method was used to investigate the comparative electrocatalytic activity of various metal oxides modified electrodes investigated in this study with CuO/MnO₂ modified electrode. MnO₂ modified electrode showed sensitivity of 0.10 μA μM⁻¹ cm² in the concentration range of 40 μM–250 μM (Fig. S7, ESI†). The intercept of the calibration curve was not found to be zero, suggesting undesired non-Faradaic processes (Fig. S7 inset, ESI†).¹⁴ However, when the similar study was performed at CuO and bare glass carbon electrode in the presence of lindane, it did not show an increment in the reduction peak, suggesting no electrocatalytic activity for lindane reduction. The limit of detection was calculated by using IUPAC (International Union of Pure and Applied Chemistry) definitions, using standard approach of alternative (SA).¹⁵

$$\text{LOD}_{\text{SA}} = 3S/q \quad (1)$$

where S is the standard deviation of the blank signal, and q is the slope of the calibration curve. Based on these observations, one can easily conclude that among the materials investigated in this study, CuO/MnO₂ modified electrode exhibited the highest activity towards lindane reduction. Fig. S8 (ESI†) shows a comparison of the DPVs obtained at CuO/MnO₂ and MnO₂ modified electrodes in the presence of 200 μM lindane. DPV measurements show that CuO/MnO₂ modified electrode exhibits higher current response compared to MnO₂ modified electrode. The current responses for 200 μM lindane at CuO/MnO₂, and MnO₂ modified electrodes are

-9.6 μA , and -8.4 μA , respectively (Fig. S8, ESI†). This improved analytical performance of CuO/MnO₂ is attributable to the synergistic contributions of the two nanostructured components in the composite. The sensing ability of the prepared CuO/MnO₂ modified electrode towards lindane was compared with the reported nanostructures (Table S2). The analytical performance of CuO/MnO₂ modified electrode is superior to the reported literature (Table S2), which are attributed to the greater number of catalytic active sites available in the CuO/MnO₂.

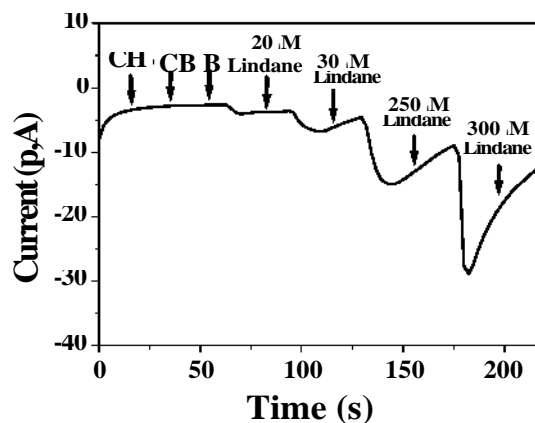


Fig. 3 Continuous amperometric response at CuO/MnO₂ modified electrode in the presence of high concentration of interfering species, such as cyclohexane (1 mM), chlorobenzene (1 mM) and benzene (1 mM) as compared to the successive addition of lindane.

The interference study was carried out using continuous amperometry. The possibility of the interference was evaluated against several inorganic ions and organic compounds (1 mM each) such as cyclohexane (CH), chlorobenzene (CB), and benzene (B) (Fig. 3). The results indicate that CuO/MnO₂ based sensor is specific to lindane. No interference was observed for 20 fold excess of triclosan, 1,3,5-trichlorobenzene (1,3,5-TCB), 4-chlorobenzaldehyde (4-CBA). It may further be noted that the response current decreased by 13.8%, when 250 times higher concentration of 1,3,5-TCB was added. It should be noted that neither ethanol (1 mM), nor phenol (1 mM) elicited any response, these compounds being picked on the grounds of water solubility and structural features. The ionic makeup of other anions likely to be present such as sulfate (1 mM) or nitrate (1 mM), and 100 fold of NH₄⁺, K⁺, Na⁺, Ca²⁺, Mn²⁺, Fe²⁺ and Co²⁺ has no effect on the peak currents corresponding to the lindane reduction signal. The reproducibility of CuO/MnO₂ was evaluated by parallel DPV investigations of five numbers of identically fabricated CuO/MnO₂ electrodes. The sensor electrodes show relative standard deviations (RSD) of only ~ 2.4%, which is significantly lower. This essentially suggests very high reproducibility of the CuO/MnO₂ modified electrode and the process of electrode fabrication, which may be crucial for the most precise estimation of lindane, which is attributed to the structural stability and non-deformity of the designed pore architecture. Stability of the sensor electrode for a longer duration is of paramount importance for better practical and economic viability. In this context, the CuO/MnO₂ based sensor electrode was subjected to sensitivity assessment over a period of 21 days at a time interval of three days. The electrode was stored at room temperature when not in use and reactivated by dipping in supporting electrolyte for 30 minutes before sensitivity measurement. A minimal sensitivity loss of ~ 1.5 % over a period of 21 days of analysis clearly showing the exceptional stability of the CuO/MnO₂ electrode, which is highly

suitable for longer duration applications. In order to verify the feasibility of the CuO/MnO₂ modified electrode, this electrochemical method was applied to determine the concentration of lindane in tap water samples. Because the content of lindane in tap water was very low, therefore, samples containing a different amount of lindane were prepared in 60:40 (v/v) methanol–tap water (20 mL) (Table S3). The RSD and recovery calculations indicated the potential practical application of our proposed sensor.

In summary, we have presented a simple and well performing novel non-enzymatic sensor for lindane. CuO/MnO₂ nano-microstructure allows a detection concentration of lindane as low as 4.8 nM. This proposed electrochemical sensing methodology is thus expected to open opportunities for the detection of lindane in the ground water and other water bodies.

This work was supported by MOE Tier 1 Grants (RGT8/13 and RG13/13) of Singapore. Authors thank the Facility for Analysis, Characterisation, Testing and Simulation (FACTS) in Nanyang Technological University for materials characterizations.

Notes and references

School of Materials Science and Engineering, Nanyang Technological University, 50 Nanyang Avenue, Singapore 639798, Singapore. E-mail: xuzc@ntu.edu.sg

† Electronic Supplementary Information (ESI) available: [Experimental details, supplementary figures]. See DOI: 10.1039/c000000x/

- 1 A. J. Durie, A. M. Z. Slawin, T. Lebl and D. O' Hagan, *Angew. Chem. Int. Ed.*, 2012, **51**, 10086.
- 2 T. M. Phillips, A. G. Seech, H. Lee and J. Trevors, *Biodegradation*, 2005, **16**, 363.
- 3 B. R. Garrido, T. A. L. Chau, G. Feijoo, F. Macias and M. C. Monterroso, *Environ. Sci. Technol.*, 2010, **44**, 7063.
- 4 S. Li, D. W. Elliott, S. T. Spear, L. Ma and W. -X. Zhang, *Crit. Rev. Environ. Sci. Technol.*, 2011, **41**, 1747.
- 5 S. L. Simonich and R. A. Hites, *Science*, 1995, **269**, 1851.
- 6 (a) M. Oturan, N. Oturan, C. Lahitte and S. Trevin, *J. Electroanal. Chem.*, 2001, **507**, 96; (b) G. Liu and Y. Lin, *Anal. Chem.*, 2005, **77**, 5894.
- 7 M. U. Anu Prathap, A. K. Chaurasia, S. N. Sawant and S. K. Apte, *Anal. Chem.*, 2012, **84**, 6672.
- 8 (a) J. P. Merz, B. C. Gamoke, M. P. Foley, K. Raghavachari and D. G. Peters, *J. Electroanal. Chem.* 2011, **660**, 121; (b) A. A. Peverly, J. A. Karty and D. G. Peters, *J. Electroanal. Chem.* 2013, **692**, 66; (c) M. U. Anu Prathap and R. Srivastava, *Electrochim. Acta*, 2013, **108**, 145; (d) A. Kumaravel, S. Vincent and M. Chandrasekaran, *Anal. Methods*, 2013, **5**, 931; (e) P. R. Birkin, A. Evans, C. Milhano, M. I. Montenegro and D. Pletcher, *Electroanalysis*, 2004, **16**, 583; (f) L. Rotariu, O. M. Istrate and C. Bala, *Sens. Actuators, B*, 2014, **191**, 491; (g) P. C. Pandey, S. Upadhyay, I. Tiwari and V. S. Tripathi, *Sens. Actuators, B*, 2001, **72**, 224.
- 9 J. F. Rusling, T. F. Connors, and A. Owlia, *Anal. Chem.*, 1987, **59**, 2123.
- 10 (a) C. Chen, Q. Xie, D. Yang, H. Xiao, Y. Fu, Y. Tan and S. Yao, *RSC Advances*, 2013, **3**, 4473; (b) C. Wei, L. Yu, C. Cui, J. Lin, C. Wei, N. Mathews, F. Huo, T. Sritharan and Z. Xu, *Chem. Commun.*, 2014, **50**, 7885; (c) M. U. Anu Prathap,

- V. Anuraj, B. Satpati and R. Srivastava, *J. Hazard. Mater.*, 2013, **262**, 766.
- 11 M. U. Anu Prathap and R. Srivastava, *Nano Energy*, 2013, **2**, 1046.
- 12 A. A. Isse, L. Falciola, P. R. Mussini and A. Gennaro, *Chem. Commun.*, 2006, 344.
- 13 (a) D. G. Peters, in *Organic Electrochemistry*, ed. H. Lund and O. Hammerich, Marcel Dekker, New York, 4th edn., 2000, ch. 8, pp. 341–377; (b) S. M. Kulikov, V. P. Plekhanov, A. I. Tsyganok, C. Schlimm and E. Heitz, *Electrochim. Acta* 1996, **41**, 527.
- 14 E. Grygolowicz-Pawlak and E. Bakker, *Electrochem. Commun.*, 2010, **12**, 1195.
- 15 J. Mocak, A. M. Bond, S. Mitchell and G. Scollary, *Pure Appl. Chem.*, 1997, **69**, 297.